

The plutonium-oxygen phase diagram in the 25-900°C range: non-existence of the $\text{PuO}_{1.515}$ phase

John M. Haschke, Long N. Dinh^{*}, William McLean II

Lawrence Livermore National Laboratory, Livermore, CA 94551, USA

^{*}Corresponding author. Address: Lawrence Livermore National Laboratory, 7000 East Avenue, Mail Stop: L-091, Livermore, CA 94551, USA. Tel.: +1 925 422 4271. E-mail address: Dinh1@llnl.gov (L. N. Dinh).

Abstract

Evaluation of data for phases formed in the Pu-O system at temperatures below 900°C shows that the observed oxides are not at equilibrium. Results are consistent with coexistence of a hexagonal solid solution (hex- $\text{PuO}_{1.5+z}$, $0 \leq z \leq 0.010$) and a cubic phase (cub- $\text{PuO}_{1.60}$) in equilibrium at 800 °C, but fail to confirm that the O/Pu ratio of the body-centered-cubic (bcc) oxide formed near the sesquioxide composition is 1.515 (1.52) or that bcc- $\text{PuO}_{1.515}$ is formed by the peritectic reaction of hex- $\text{PuO}_{1.510}$ with cub- $\text{PuO}_{1.60}$. Stable Pu(IV)/Pu(III) ratios observed for products of the Pu- H_2O reaction correspond to members of the $\text{Pu}_n\text{O}_{2n-2}$ homologous series, but a product is not formed at O/Pu = 1.515. Metastable bcc- $\text{PuO}_{1.50}$ ($n = 4$) and stable hex- $\text{PuO}_{1.5+z}$ coexist below 285 °C, the point at which reversible eutectic decomposition of cubic $\text{PuO}_{1.60}$ ($n = 5$) produces a non-equilibrium mixture of bcc- $\text{PuO}_{1.50}$ and sub-stoichiometric dioxide (PuO_{2-y}). Transformation of bcc- $\text{PuO}_{1.50}$ to stable hex- $\text{PuO}_{1.50}$ and reactions of the hexagonal oxide to form higher-composition cubic phases are kinetically hindered. An alternative diagram describing non-equilibrium chemical behavior of the Pu-O system is presented.

1. Introduction

Investigation of properties and equilibria of plutonium oxides has focused on characterization of the dioxide because of its use in fabrication of mixed-oxide fuel. PuO_2 is the only detectable surface phase on the metal in air at room temperature, but phase diagrams for plutonium-oxygen [1, 2] show that Pu should coexist with the hexagonal sesquioxide (hex- Pu_2O_3 or $\beta\text{-Pu}_2\text{O}_3$), not the kinetically favored dioxide [3]. Heating of dioxide-coated metal in vacuum or an inert atmosphere forms a Mn_2O_3 -type body-centered-cubic (bcc) surface oxide [3, 4] with crystallographic properties like those of Mn_2O_3 -related $\text{PuO}_{1.515}$ ($\text{PuO}_{1.52}$ or $\alpha\text{-Pu}_2\text{O}_3$) described in the seminal x-ray-diffraction (XRD) study of samples prepared by reducing dioxide at high temperature [5]. That study and a companion thermodynamic investigation [6] form the basis for the accepted Pu-O phase diagram below 900 °C.

Interest in the Mn_2O_3 -related surface oxide has increased significantly due to recent studies showing that the bcc phase drives self-sustained oxidation of the metal at high temperatures [7] and catalytically promotes the corrosion of plutonium by hydrogen, oxygen, and air [3,8-10]. Exposure of hydride coated Pu to O_2 forms a bcc- Pu_2O_3 surface layer and increases the Pu oxidation rate by a factor of 10^{10} . Catalytic behavior is supported by a-priori calculations showing that the dissociation reactions of adsorbed H_2 and O_2 are promoted by 5d electrons of Pu(III) and have activation energies near zero [11]. If the surface oxide is $\text{PuO}_{1.515}$ ($(\text{Pu(III)})_{1.94}\text{Pu(IV)}_{0.06}\text{O}_{3.03}$), the effects of Pu(IV) on catalysis should be considered. Rapid transport of dissociated reactants through the catalytic bcc- Pu_2O_3 product layer is necessary to account for the observed oxidation rates [3].

Here, we evaluate diverse experimental data relevant to equilibria of oxides existing near the sesquioxide composition and at temperatures below 900 °C. In large measure, our effort utilizes the high-temperature XRD data of Gardner et al. [5] for oxides prepared by H₂ reduction of PuO₂ and the chemistry of Pu oxidation by liquid water at room temperature [12, 13]. Those studies are augmented by comparison to analogous lanthanide systems [14] and by XRD results for surface oxides formed by heating PuO₂-coated α -phase [4] and δ -stabilized [15] metal in inert atmospheres. The assessment is facilitated by application of crystal chemistry in evaluating diffraction data and identifying non-equilibrium processes. Inconsistencies between observations and the accepted Pu-O phase diagram are discussed and an alternative description of the system is proposed.

2. Experimental bases for reevaluation of the Pu-O system

Evaluation of equilibria in the Pu-O system relies on x-ray diffraction data for oxide products from diverse sources. In the study by Gardner et al. [5], pelletized PuO₂ was reduced by H₂ at 1520°C or by H₂ and Pu at 1500 °C. After part of the product was oxidized to determine the bulk composition (\pm 0.005 uncertainty in O/Pu), remaining pellets were reacted with volumetrically measured amounts of O₂ at 800°C to prepare XRD samples with desired O/Pu ratios. The reported O/Pu ratios of samples are accepted unless contradicted by credible observations. XRD data were obtained during stepwise heating of cooled products to 900 °C in sealed quartz capillaries. Pt was used both as internal standard and as a temperature standard. Subsequent reinvestigation showed that the temperatures reported initially were too low by $35 \pm 5^\circ\text{C}$ [6] and all values are corrected accordingly.

The compositions of phases formed during oxidation of high-purity α -phase Pu by water at 25°C were determined by quantifying the time-dependence of H₂ formation over a year-long period [3, 12, 13]. A linear time dependence of the H₂/Pu ratio for the initial reaction of Pu and a progressively lower slope for each subsequent product implies that the rates of reaction were under equilibrium control. The Pu(IV)/Pu(III) ratios of stable product phases were defined by the intersection points (± 0.002 in anion/Pu ratio) of successive H₂/Pu-time lines. The average deviation of O/Pu ratios from ideal values for known lanthanide oxide analogs is ± 0.005 .

Lattice parameters of the bcc oxide formed by auto-reduction of the dioxide layer on Pu were calculated using 2θ values obtained for high-purity α -phase metal from high-temperature XRD spectra published by Terada et al. [4] and at for δ -phase Ga alloy from room temperature spectra measured after samples had been reacted at 350-500°C in He or Ar [15]. Values for unalloyed Pu were derived from diffraction spectra measured during heating in vacuum (10^{-7} mbar) and in low-pressure (3 mbar) O₂ [4]. Values for a_0 at 305 and 420°C agree (± 1 pm) with parameters for bulk oxide samples at those temperatures. Lattice parameters for the bcc oxide at 25 °C were obtained using the reported thermal expansion coefficient of $9 \times 10^{-6} \text{ }^\circ\text{C}^{-1}$ [5].

3. Assessment of the current Pu-O phase diagram

The XRD study by Gardner et al. [5] is the most extensive and reliable basis for describing equilibria in the plutonium-oxygen system at temperatures below 900 °C. The relevant region of the O-Pu diagram proposed by these workers (Figure 1) shows phase relationships that are still accepted and included in recent reviews of the system [1,2]. The complexity of Figure 1 results from identification of an oxide phase at O/Pu = 1.515. Our analysis of data presented by

Gardner et al. shows that Figure 1 is at variance with their published data and does not support the existence of $\text{PuO}_{1.515}$.

In order to minimize the confusion resulting from a plethora of terminology used to identify the oxide phases [1], the formulae in Figure 1 specify both the lattice symmetry and the O/Pu ratio. A hexagonal La_2O_3 -related oxide observed up to 900°C is identified here as hex- $\text{PuO}_{1.510}$. A body-centered-cubic Mn_2O_3 -related oxide observed at O/Pu=1.515 and coexisting with hex- $\text{PuO}_{1.510}$ at temperatures below 450°C is designated as bcc- $\text{PuO}_{1.515}$. In the 25 - 335°C range, a two-phase region is formed by bcc- $\text{PuO}_{1.515}$ and a CaF_2 -related oxide identified as cub- PuO_{2-y} . At 335°C , these oxides combine in a reverse eutectic reaction to form cub- $\text{PuO}_{1.61}$, another CaF_2 -related oxide. The diagram shows that bcc- $\text{PuO}_{1.515}$ and cub- $\text{PuO}_{1.61}$ coexist in a two-phase region above 335°C until the bcc oxide decomposes peritectically to form hex- $\text{PuO}_{1.510}$ and additional cub- $\text{PuO}_{1.61}$ at 450°C . The cub- $\text{PuO}_{1.61}$ oxide is the terminal ($y = 0.39$) composition of the PuO_{2-y} solid solution. The full diagram presented by Gardner et al. [5] shows that PuO_{2-y} extends from O/Pu = 1.61 to O/Pu=2.0 with closure of the miscibility gap near 700°C . Two cubic PuO_{2-y} phases (designated 1 and 2) with different y values coexist in the gap above the 335°C eutectic reported for cub- $\text{PuO}_{1.61}$.

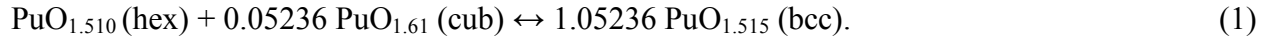
The 1.515 O/Pu ratio reported for the bcc oxide by Gardner et al. [5] is based on the a_0 value measured at 25°C and a complicated Vegard's law procedure, not on chemical analysis. XRD results show that a_0 of PuO_{2-y} varies linearly with O/Pu at constant temperature in compliance with Vegard's law and with temperature due to the thermal expansion at constant O/Pu. Values of a_0 for fixed O/Pu ratios of a hypothetical PuO_{2-y} phase at 25°C were determined by extrapolating experimental a_0 -temperature equations to room temperature and were used to

derive a Vegard's law equation ($a_o = A - B(\text{O/Pu})$) for the theoretical solid solution at 25°C. Gardner et al. assumed that O/Pu of the bcc oxide is accurately defined by this equation and a_o .

Use of A (1.1753nm) and B (0.0464 nm) values extracted from the published a_o -O/Pu graph for 25°C [5] and the average a_o of 1.105nm (1.1045 ± 0.0012 , 2σ uncertainty) reported for the bcc oxide at 25°C gives the 1.515 ratio, but does not show the composition range ($1.493 \leq \text{O/Pu} \leq 1.537$) defined by including the uncertainty (± 0.001 nm) in a_o . Values of A and B (1.1702 ± 0.0046 nm and 0.0434 ± 0.0027 nm, respectively) obtained by least-squares analysis of the digitized a_o -O/Pu data for 25°C give an O/Pu ratio of 1.502 ± 0.025 . Repetition of the Vegard's-law method in determining O/Pu for the cubic oxide coexisting with hex-PuO_{1.510} gives a comparably uncertain result (1.597 ± 0.019). Inclusion of the 35°C correction in the temperature measurement decreases A values by 0.001 nm and lowers all calculated O/Pu ratios by more than 0.02. Reliable determination of oxide compositions via the Vegard's law method of Gardner et al. [5] is precluded by uncertainties in the lattice parameters and temperature.

The consistency of Figure 1 with XRD results reported by Gardner et al. [5] is examined (Table 1) by comparing observations for experimental O/Pu ratios and temperatures with phase-diagram-based predictions for those conditions. As indicated by the diagram, diffraction data show coexistence of hex-PuO_{1.510} with cub-PuO_{1.61} for all O/Pu ratios between 1.51 and 1.61 at temperatures above 450°C. Lattice parameters for the single phase product observed at O/Pu = 1.510 are consistent with thermal expansion of a fixed-composition phase over the 25-890°C range. This result and the coexistence of hex-PuO_{1.510} and cub-PuO_{1.61} above 450°C for O/Pu ratios between 1.51 and 1.61 are the only reported XRD results that agree with Figure 1.

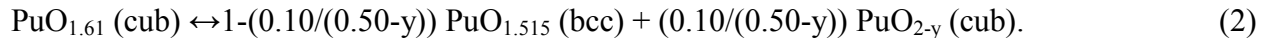
Discrepancies are observed at all experimental O/Pu ratios in the 1.51 to 1.61 range and at all temperatures below the 450°C peritectic. The XRD result for O/Pu = 1.515 below 335°C (Table 1) is especially disconcerting because the product is a triphasic mixture, not pure bcc-PuO_{1.515}. As noted in the report [5], the XRD results do not show either the hex-PuO_{1.510} + bcc-PuO_{1.515} or bcc-PuO_{1.515} + cub-PuO_{1.61} two-phase regions. Existence of these phase fields is contingent on occurrence of Equation 1 at 450°C as hex-PuO_{1.510} + cub-PuO_{1.61} equilibrium mixtures are cooled:



Although complete reaction of hex-PuO_{1.510} is expected for 1.515 ≤ O/Pu ≤ 1.61, the hexagonal oxide is consistently present at 25-800°C without variation in diffraction intensity. Observations imply that hex-PuO_{1.510} and cub-PuO_{1.61} equilibrate at 800°C, but do not react to form the bcc-PuO_{1.515} + cub-PuO_{1.61} two-phase region at lower temperatures.

Since the lattice parameters and crystallographic symmetries of bcc-PuO_{1.515} and cub-PuO_{1.61} are similar, coexistence of the oxides in the 335-450°C phase field may not have been detected due to coincidence of their diffraction patterns. Examination of that possibility using data for O/Pu=1.590 [5] during stepwise heating (Figure 2) shows that the two oxides are easily distinguished by XRD.

Figure 1 shows that cub-PuO_{1.61} is observed above 335°C for all products with O/Pu in the 1.515-1.600 range. Eutectic decomposition of the phase at that temperature forms a bcc-PuO_{1.515} + cub-PuO_{2-y} mixture as described by Equation 2:



All bcc-PuO_{1.515} and cub-PuO_{2-y} formed by this reaction on cooling recombine on heating.

However, Figure 2 shows that the eutectic reaction occurs at a substantially lower temperature than reported by Gardner et al. [5].

Absence of an oxide phase at O/Pu = 1.515 is shown by results obtained during the reaction of Pu with liquid water at 25°C [3, 12, 13]. The product existing at pure Pu(III) is identified as bcc-PuO_{1.50}. Subsequent products have Pu(IV)/Pu(III) ratios identical to those for CaF₂-related praseodymium oxides [14] and are identified as the n = 7, 9, 10, and 12 members of the Pu_nO_{2n-2} homologous series [12,13]. The difference between the Pu(IV) percentages for the n=9 and n=10 members of the homologous series (4.4%) is easily discernable and comparable to that (3.0%) for the 1.500 and 1.515 O/Pu ratios. Evidence is not found for formation of any phases between PuO_{1.50} (n = 4) and PuO_{1.714} (n = 7) at 25°C.

Additional similarities of the trivalent oxides formed by Pr, Nd, and Pu are evidenced by the comparison of crystallographic data in Table 2. Agreement of lattice symmetries and parameters is observed, but the 1.515 O/Pu ratio of the bcc plutonium oxide is anomalous. The bcc Mn₂O₃-type structure is derived from the CaF₂-type parent by formation and ordering of vacancies **on one-fourth of the anion sites, a process that changes the space group from Fm3m to Ia3 with** $a_0(\text{bcc}) = 2 a_0(\text{fcc})$ [16]. The bcc superstructure is characteristic of the stoichiometric phases; the likelihood of its observation for a non-ideal Pu(III)_{0.97}Pu(IV)_{0.03}O_{1.515} phase containing excess oxygen is uncertain.

4. Derivation of an alternative Pu-O diagram

As shown in Section 3, the Pu-O system is not accurately described by the accepted diagram in Figure 1. Consideration of an alternative description of the Pu-O system is merited. Four oxides exist in the temperature-composition range of interest. Attainment of equilibrium in

the system is difficult at low temperatures due to kinetic control of reaction pathways by crystal chemistry of the oxides.

Three of the oxides are structurally related to CaF_2 -type PuO_2 and chemically related as participants in the reversible eutectic reaction observed near 285°C (Figure 2). The PuO_{2-y} decomposition product is a non-stoichiometric phase with disordered oxygen vacancies and compositions confined to the oxygen-rich boundary of miscibility gap. As in the $\text{Pu}_n\text{O}_{2n-2}$ homologous-series oxides [3, 12, 13], oxygen vacancies in the Mn_2O_3 -type structure of the other product are ordered. The phase is identified as bcc- $\text{PuO}_{1.50}$, the stoichiometry observed at pure Pu(III) during water oxidation and defined by $n = 4$ of the homologous series. Within the range of analytical uncertainty [5], the terminal composition of the cubic solid solution corresponds to the $n = 5$ member of the series and is identified as cub- $\text{PuO}_{1.60}$.

The remaining oxide of interest is the hex- $\text{PuO}_{1.5+z}$ solid solution observed in 1.500-1.510 O/Pu range [5]. The La_2O_3 -type parent structure is based on a hexagonal-closest-packed (hcp) array of oxide ions in layers with octahedral (trigonal antiprism) vacancies between the layers normal to a_0 [16]. Two thirds of the octahedral sites in the hexagonal array are occupied by Pu(III). The hexagonal solid solution is derived by replacement of Pu(III) with Pu(IV) and concurrent occupation of vacant octahedral sites by O^{2-} . The phase is identified as hex- $\text{PuO}_{1.5+z}$ ($0 \leq z \leq 0.010$).

Unlike hex- $\text{PuO}_{1.5+z}$, bcc- $\text{PuO}_{1.50}$ apparently exists in a narrow composition range because the observed variation in a_0 (Table 3) is $\pm 2\%$, a value typical of independent XRD results.

Formation of CaF_2 -related oxides during reduction of PuO_2 and during oxidation of δ -phase Pu at 350 and 420°C [4] is not surprising because Pu atoms pre-exist in fcc arrays before reaction.

Hexagonal La_2O_3 -type oxide is the stable phase coexisting with Pu [17], and its formation might be expected during oxidation of the α , β , and γ polymorphs. Results for 170 and 305°C (Table 3) show that bcc oxide forms on β - and γ -Pu [4] and that CaF_2 -related products form during reaction of α -Pu with water [12,13]. The $\alpha \rightarrow \beta$, $\beta \rightarrow \gamma$, and $\gamma \rightarrow \delta$ transitions occur at 122, 207, and 315°C, respectively, with corresponding enthalpies of 3.4, 1.2 and 1.0 kJ mol^{-1} [18]. Such facile changes are consistent with displacive phase transitions that occur between closely related structures and allow Pu atoms in other polymorphic forms to acquire the non-equilibrium fcc (δ -phase) arrangement during oxidation.

The difficulty of defining the equilibrium diagram for Pu-O is increased by existence of two oxides at $\text{O/Pu} = 1.50$ and the need to determine which form is thermodynamically stable. Rerequisite thermodynamic data for bcc- $\text{PuO}_{1.50}$ and the hexagonal Pu-O solid solution are unavailable. However, evaluation of Gibbs energy data [19] by graphing $\Delta G^\circ_f (\text{Ln}_2\text{O}_3)$ versus atomic number for light lanthanides shows two parallel lines with a negative slope. The spacing of the lines for Ln_2O_3 -type (La, Ce, Pr) and Mn_2O_3 -type (Nd, Sm) sesquioxides shows that La_2O_3 -type oxides are $30 \pm 5 \text{ kJmol}^{-1}$ more stable than the Mn_2O_3 -type oxides at 25°C. The only reason for a difference in the amounts of energy released during formation of the hexagonal and cubic oxides is the difference in lattice energy as determined by the structure and the anion-cation distances. Agreement of the structures and lattice parameters for plutonium and the lanthanide oxides (Table 2) implies that hex- $\text{PuO}_{1.50}$ is more stable than bcc- $\text{PuO}_{1.50}$, a result that is consistent with the substantially greater theoretical density for the hexagonal oxide (11.48 g.cm^{-3}) relative to that for the cubic form (10.37 g.cm^{-3}).

The kinetics of oxygen transport and phase transition in the hexagonal and cubic oxides are important in determining phase relationships of the Pu-O system. In both structures, transport

occurs by diffusion of O^{2-} via vacant octahedral sites. The transport rate in PuO_2 is slowed by layers of oxygen parallel to (100), but increases as the anion vacancy concentration in cub- PuO_{2-y} increases with increasing y . The potential for maximum transport exist for bcc (Mn_2O_3 -type) because ordering of vacancies forms infinite oxide-free channels [16] that provide a pathway for unobstructed transport of O^{2-} . Relatively slow diffusion of O^{2-} is also expected for stoichiometric hex- $PuO_{1.50}$. But, unlike the cubic oxide, transport and composition change become increasingly difficult as z increases and the concentration of vacant octahedral sites in hex- $PuO_{1.5+z}$ decreases. In the composition and temperature range of interest, transport-driven bulk composition changes in cubic CaF_2 -related oxides are relatively facile compared to the self-limiting behavior encountered with La_2O_3 -related hex- $PuO_{1.5+z}$. Phase transitions and reactions between CaF_2 - and La_2O_3 -related phases are anticipated only at elevated temperatures where thermal energy is sufficient for reordering of metal atoms between the cubic and hexagonal arrays of those structures. **Although formation of the metastable bcc oxide is consistent with crystallographic properties, the effect of radiation on the process is unknown.**

As implied by the preceding discussion of oxide crystal chemistry, attainment of equilibrium in the Pu-O system is possible only if the temperature is sufficiently high for reordering of the metal atoms. XRD results [5] show that this condition is satisfied during sample preparation at 800°C because hex- $PuO_{1.510}$ is progressively replaced by cub- $PuO_{1.60}$ as O/Pu of the reaction mixture is increased. The apparent solubility limit of oxygen in the hexagonal solid solution is at $z = 0.010$. Except for the decrease in a_0 described by thermal expansion, XRD data remain unchanged during cooling to 25°C and step-wise heating to 800-900°C. Failure to form bcc- $PuO_{1.515}$ by peritectic reaction (equation 1) or to detect an anticipated decrease in z at low temperature is consistent with the kinetic limitation on reordering of Pu into the cubic lattice of a

product phase. In contrast to lack of chemical involvement by the hexagonal oxide, cub-PuO_{1.60} disproportionates near 285°C (Figure 2) via a reversible reaction to form bcc-PuO_{1.50} and cub-PuO_{2-y}. The eutectic reaction is both thermodynamically and kinetically favorable, but bcc-PuO_{1.50} is a metastable product. Movement of oxide ions simultaneously forms intra-granular regions of low oxygen concentration (bcc-PuO_{1.50}) and high oxygen concentration (cub-PuO_{2-y}) during cooling and reverses the process to reform cub-PuO_{1.60} upon heating to the eutectic temperature. The reaction is described by Equation 2 if oxide compositions are modified by replacing 1.61 with 1.60 and 1.515 with 1.50.

The plutonium-oxygen diagram in Figure 3 is proposed as a replacement for Figure 1. In large measure, the diagram shows kinetically controlled chemical relationships of plutonium oxide phases, not equilibrium relationships. Although some investigators report that the cubic phase near O/Pu = 1.60 is discrete [1], the oxide is accurately described as the terminus of the cub-PuO_{2-y} solid solution at the composition defined by $n = 5$ of the Pu_nO_{2n-2}. That conclusion is supported by a recent analysis of data for the cub-PuO_{2-y} solid solution [20]. The relationship between hex-PuO_{1.50} and bcc-PuO_{1.50} is implied by identification of hexagonal oxide as the stable phase. The transition temperature is unknown, but is bracketed by formation of the bcc oxide at 420°C (Table 3) and the hexagonal oxide at 800°C. Transformation of bcc Nd₂O₃ to the hexagonal form is observed near 600°C [14] and similar behavior is anticipated for bcc-PuO_{1.50}. The consistency of the alternative diagram with published XRD results [5] is shown (Table 4) by agreement of observations and predictions for all experimental O/Pu ratios and temperatures.

5. Conclusions

Understanding of chemical behavior in the Pu-O system at low temperatures and low O/Pu ratios is enhanced by results of this study. Path dependence is evident because behavior of products prepared by high-temperatures reduction of PuO₂ [5] differs markedly from that of products obtained by aqueous oxidation at room temperature [13]. Equilibrium is established during oxide reduction, but is not maintained at low temperatures because formation of bcc-PuO_{1.50} is kinetically favored by facile O²⁻ transport in CaF₂-related phases and by absence of sufficient thermal energy for reordering Pu atoms into a more stable La₂O₃-related structure. Equilibrium is also not attained during oxidation of Pu metal because formation of Ca-F₂-related oxides is kinetically more favorable than formation of the stable hexagonal sesquioxide. A second alternative diagram based on results of the Pu-H₂O reaction [3] is similar to those of Ce-O and Pr-O with phase fields bounded by CaF₂-related homologous-series oxides (n = 4, 7, 9, 10, 12, and ∞). Phase behavior of those oxides at elevated temperatures is speculative. Attainment of equilibrium in the Pu-O system appears unlikely if the hexagonal oxide is the stable phase at O/Pu = 1.50.

Acknowledgement

This work was performed under the auspices of the U.S. Department of Energy by Lawrence Livermore National Laboratory under Contract DE-AC52-07NA27344.

References

- 1) H.A. Wreidt, Bull. Alloy Phase Diagr. 11 (1990) 184.
- 2) R.J. Lemire, J. Fuger, H. Nitsche, P. Potter, M.H. Rand, J. Rydberg, K. Spahiu, J.C. Sullivan, W.J. Ullman, P. Vitorge, H. Wanner, Chemical Thermodynamics of Neptunium and Plutonium, Elsevier, Amsterdam, 2001, 331-332.

- 3) J.M. Haschke J.L. Stakebake, The Chemistry of the Actinide and Transactinide Elements, Vol. 5, L.R. Morss, N.M. Edelstein, J. Fuger, Springer, 2006, 3199-3272.
- 4) K. Terada, R.L. Meisel, M.R. Dringman, J. Nucl. Mater. 30 (1969) 340.
- 5) E.R. Gardner, T.L. Markin, R.S. Street, J. Inorg. Nucl. Chem. 27 (1965) 541.
- 6) T.L. Markin, M.H. Rand, Proceedings of the Symposium on Thermodynamics: Vol. 1, International Atomic Energy Agency, Vienna, 1966, 145-156.
- 7) J.M. Haschke, J.C. Martz, J. Alloys. Compds. 266 (1997) 81.
- 8) J.M. Haschke, T.H. Allen, L.A. Morales, Los Alamos Science 26, Los Alamos National Laboratory, 2000, pp. 252-273.
- 9) L.N. Dinh, J.M. Haschke, C.K. Saw, P.G. Allen, W. McLean II, J. Nucl. Mater. 408 (2011) 171.
- 10) J. M. Haschke, T.H. Allen, J. Alloys Compds. 320 (2001) 58.
- 11) K. Balasubramanian, personal communication, Livermore National Laboratory, 2013.
- 12) J. M. Haschke, A. E. Hodges III, G. E. Bixby, R.L. Lucas, USDOE Report RFP-3416, Rocky Flats Plant, Golden, CO, 1983.
- 13) J. M. Haschke, Transuranium Elements. A Half Century Ch. 40, American Chemical Society, Washington, DC, 1992, 416-425.
- 14) L. Eyring, Handbook on the Physics and Chemistry of Rare Earths, Vol. 3, North-Holland, Amsterdam, 1979, 337-399.

- 15) J.M. Haschke, XRD data collected at the Rocky Flats Plant, Golden, CO and Los Alamos National Laboratory, Los Alamos, NM.
- 16) A.F. Wells, Structural Inorganic Chemistry, Oxford University Press, London, 1975, 450-452.
- 17) T.D. Chikalla, C.E. McNeilly, R.E. Skavdal, J. Nucl. Mater, 12 (1964) 131.
- 18) F.L. Oetting, M.H. Rand, R.J. Ackermann, The Chemical Thermodynamics of Actinide Elements and Compounds: Part 1, International Atomic Energy Agency, Vienna, 1976, 24.
- 19) K.A. Gschneidner, N. Knippenman, D.D. McMaster, USDOE Report IS-RIC-6, Iowa State University, Ames, IA (1973).
- 20) C. Guénau, N. Dupin, B. Sundman, C. Martial, J-C Dumas, S. Gossé, S. Chatain, F. De Bruycker, D. Manara, R. J. M. Konings, J. Nucl. Mater. 419 (2011) 145.
-

Table 1. Comparison of phase relationships in Figure 1 with qualitative XRD results reported [5,6] for experimental O/Pu ratios and temperatures. For each O/Pu and temperature, the calculated fraction of each phase is given in the Pred. column. Phases observed by XRD are marked with an x in the Obs. column; those not detected are marked with 0.

O/Pu	Phase	Temperature Range (°C) ^a					
		<335		335-450		>450	
		Pred	Obs	Pred	Obs	Pred	Obs
1.510	hex-PuO _{1.510}	1	x	1	- ^b	1	x
	bcc-PuO _{1.515}	0	0	0	-	0	0
	cub-PuO _{1.61}	0	0	0	-	0	0
	cub-PuO _{2-y}	0	0	0	-	0	0
1.515	hex-PuO _{1.510}	0	x	0	- ^b	0.95	- ^b
	bcc-PuO _{1.515}	1	x	1	-	0	-
	cub-PuO _{1.61}	0	0	0	-	0.05	-
	cub-PuO _{2-y}	0	x	0	-	0	-
1.590	hex-PuO _{1.510}	0	x	0	x	0.20	x
	bcc-PuO _{1.515}	0.84	x	0.21	0	0	0
	cub-PuO _{1.61}	0	0	0.79	x	0.80	x
	cub-PuO _{2-y}	0.16	x	0	0	0	0

a. Temperatures in the initial report [5] are corrected by addition of 35 degrees [6].

b. XRD measurements are not reported for the experimental O/Pu in this temperature range.

Table 2. Comparison of crystallographic data for oxides of Pr, Nd, and Pu.

O/M Ratio	Lattice Symmetry	Lattice Parameter (nm) ^a			Reference
		Pr	Nd	Pu	
1.5	hex a_o c_o	0.3857 0.6016	0.3827 0.6002	0.3829 0.6001	5,14
1.5	bcc a_o	1.1152	1.1080	-- ^b	14
1.515	bcc a_o	-- ^b	-- ^b	1.105	5
2.0	fcc a_o	0.5393	-- ^b	0.5396	14,19

a. Uncertainties in the values of a_o and c_o for the oxides of Pr and Nd are less than 1% of lattice dimension.

b. This oxide composition is not observed.

Table 3. Comparison of bcc lattice parameters for bulk oxides formed by H₂ reduction of PuO₂ and for surface oxides formed by auto-reduction of PuO₂ on Pu.

Preparative and Measurement Conditions	a_o (nm)	Reference
H ₂ /Pu reduced powder, 1.5<O/Pu<1.9, formed <335 °C	1.105(1)	5
Surface oxide, Pu reduced in vacuum at 170 °C	1.104(3)	4 ^a
Surface oxide, Pu reduced in vacuum/3 mbar O ₂ at 305 °C	1.102(2)	4 ^{a,b}
Surface oxide, Pu reduced in vacuum at 350 °C	1.105(1)	4 ^{a,b}
Surface oxide, Pu reduced in vacuum at 420 °C	1.106(3)	4 ^{a,b}
Surface oxide, Pu reduced in inert gas at 350-550 °C	1.103(2)	This Study ^b

a. The lattice parameter was derived for preparative temperature using the published diffraction pattern; values at 25 °C were calculated using $\Delta l/l = 9 \times 10^{-6} \text{ } ^\circ\text{C}^{-1}$.

b. The bcc oxide coexisted with plutonium oxide carbide, PuO_{0.5}C_{0.4}.

Table 4. Comparison of phase relationships in Figure 3 with XRD results reported [5,6] for experimental O/Pu ratios and temperatures. For each O/Pu and temperature, the calculated fraction of each phase is given in the Pred. column. Phases observed by XRD are marked with an x in the Obs. column; those not detected are marked with 0.

O/Pu	Phase	Temperature Range (°C) ^a			
		<285		>285	
		Pred	Obs	Pred	Obs
1.510	hex-PuO _{1.510}	1	x	1	x
	bcc-PuO _{1.50}	0	0	0	0
	cub-PuO _{1.60}	0	0	0	0
	cub-PuO _{2-y}	0	0	0	0
1.515	hex-PuO _{1.510}	0.94	x	0.94	x
	bcc-PuO _{1.50}	0.05	x	0.06	x
	cub-PuO _{1.60}	0	0	0	0
	cub-PuO _{2-y}	0.01	x	0	0
1.590	hex-PuO _{1.510}	0.11	x	0.11	x
	bcc-PuO _{1.50}	0.70	x	0	0
	cub-PuO _{1.601}	0	0	0.89	x
	cub-PuO _{2-y}	0.19	x	0	0

a. Temperatures in the initial report [5] are corrected by addition of 35 degrees [6].

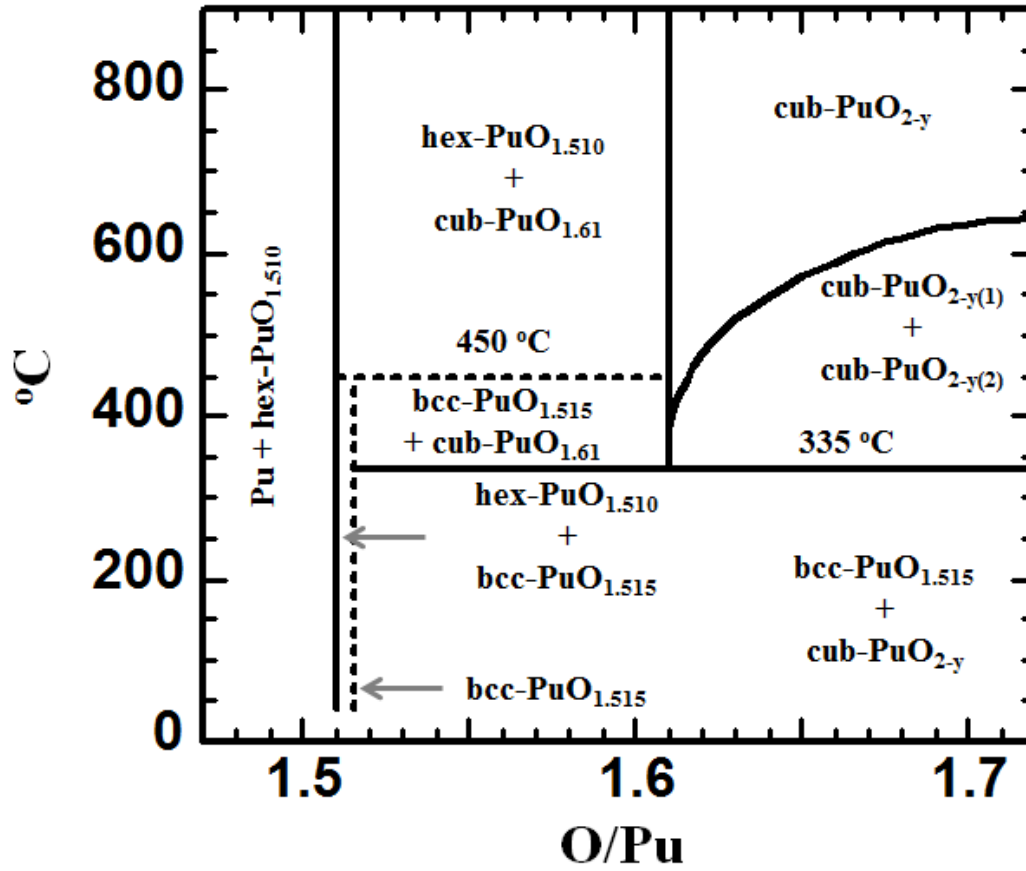


Figure 1: The partial Pu-O phase diagram for low O/Pu ratios from reports by Gardner et al. [5] and by Markin and Rand [6].

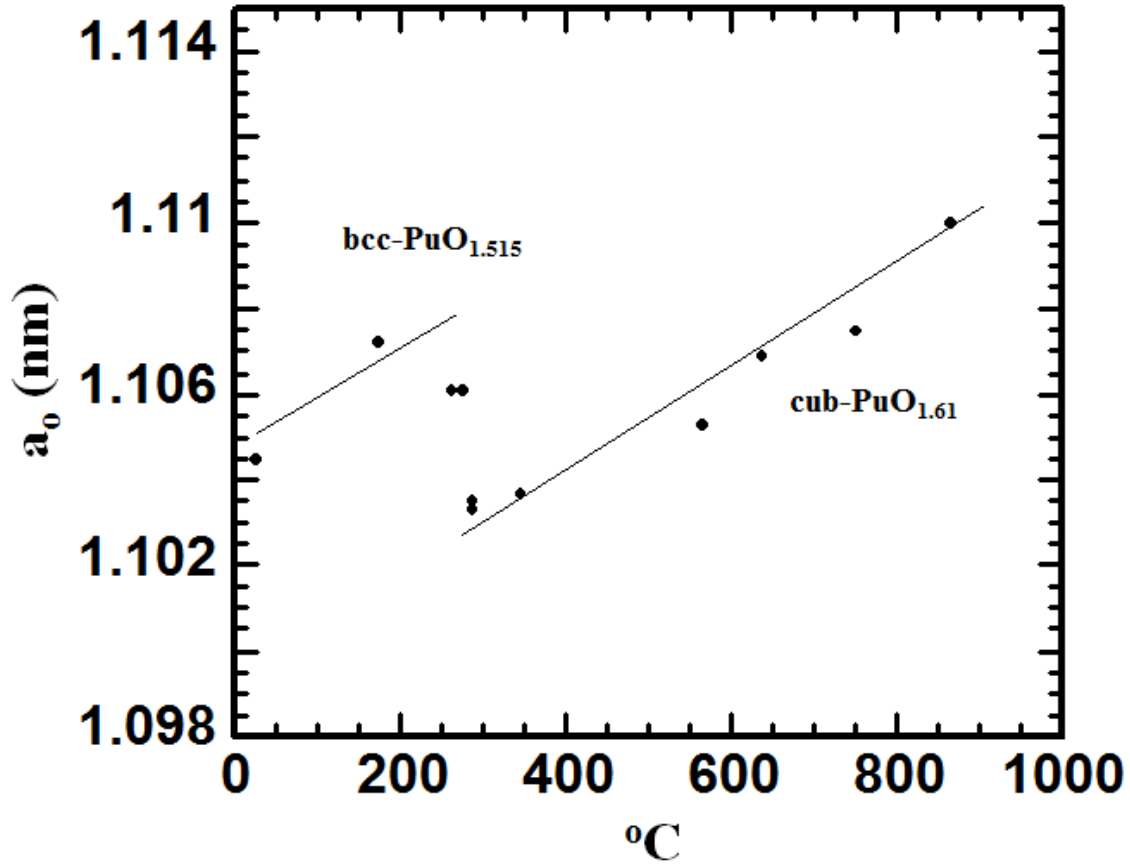


Figure 2: Temperature dependence of a_0 values measured for the bcc plutonium oxide and cub-PuO_{1.61} during heating of a sample with an O/Pu ratio of 1.590. The comparison is facilitated by use of $2 \times a_0$ (cubic cell) as the lattice parameter for cub-PuO_{1.61}. The slope of the line for 25-285°C is fixed by the thermal expansion equation for bcc-PuO_{1.515}.

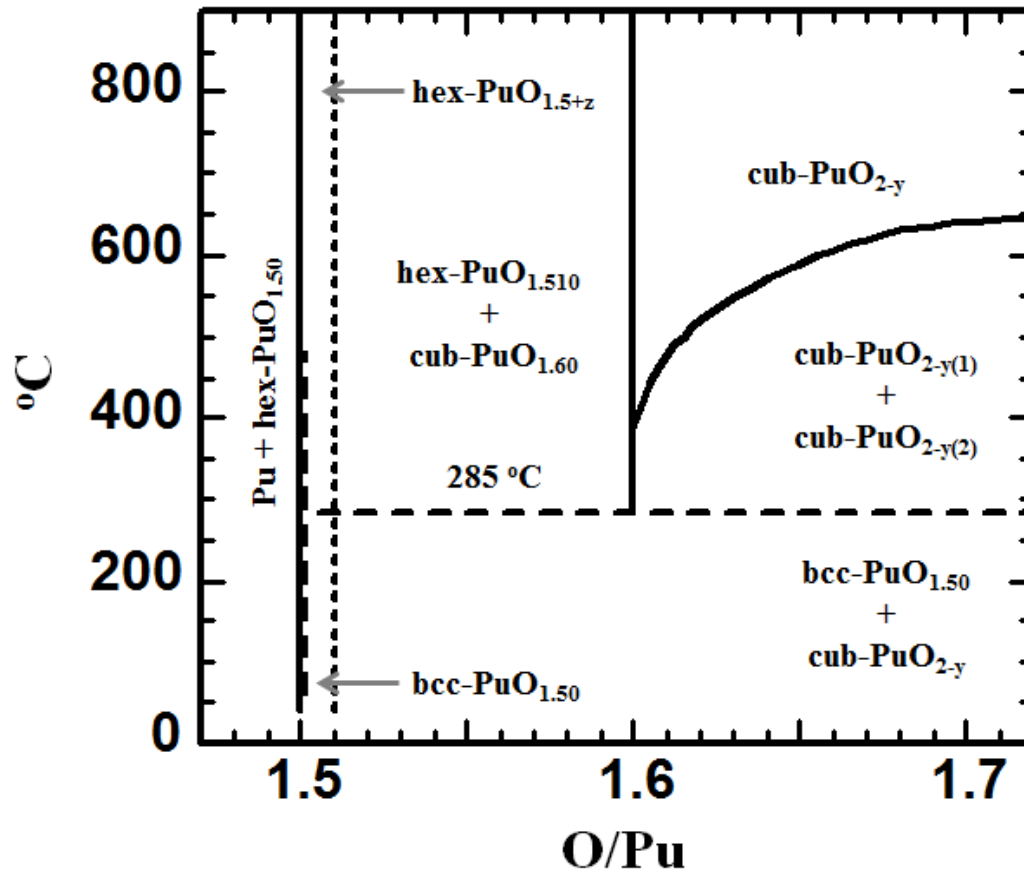


Figure 3: The proposed partial Pu-O diagram showing non-equilibrium chemical relationships of oxides formed at low O/Pu ratios. Non-equilibrium phases, phase boundaries and tie-lines are indicated by dashes. The compositions of hex-PuO_{1.50} and bcc-PuO_{1.50} coincide, but are graphed with a small separation to show the presence of both phases. Cross-over of the hex-PuO_{1.5+z} phase field by the eutectic line at 285°C is allowed because the system is not at equilibrium.